

Supersymmetric Electroweak Corrections to Sbottom Decay into Lighter Stop and Charged Higgs Boson

Li Gang Jin and Chong Sheng Li

Department of Physics, Peking University, Beijing 100871,
People's Republic of China

ABSTRACT

The Yukawa corrections of order $\mathcal{O}(\alpha_{ew}m_{t(b)}^2/m_W^2)$, $\mathcal{O}(\alpha_{ew}m_{t(b)}^3/m_W^3)$ and $\mathcal{O}(\alpha_{ew}m_{t(b)}^4/m_W^4)$ to the width of sbottom decay into lighter stop plus charged Higgs boson are calculated in the Minimal Supersymmetric Standard Model. These corrections depend on the masses of charged Higgs boson and lighter stop, and the parameters $\tan\beta$ and μ . For favorable parameter values, the corrections decrease or increase the decay widths significantly. Especially for high values of $\tan\beta(=30)$ the corrections exceed at least 10% for both \tilde{b}_1 and \tilde{b}_2 decay. But for low values of $\tan\beta(=4,10)$ the corrections are small and the magnitudes are less than 10%. The numerical calculations also show that using the running bottom quark mass which includes the QCD effects and resums all high order $\tan\beta$ -enhanced effects can improve much the convergence of the perturbation expansion.

PACS number(s): 14.80.Cp; 14.80.Ly; 12.38.Bx

1 Introduction

The Minimal Supersymmetric Standard Model (MSSM)[1, 2] is an attractive extension of the Standard Model (SM). In this Model every quark has two spin zero partners called squarks \tilde{q}_L and \tilde{q}_R , one for each chirality eigenstate. These current eigenstates mix to form the mass eigenstates \tilde{q}_1 and \tilde{q}_2 . The third generation squarks are of special interest. This is mainly due to the reasons: large Yukawa couplings lead to strong mixing which induces large mass differences between the lighter mass eigenstate and the heavier one. This implies in general a very complex decay pattern of the heavier states. The dominate decay modes of the heavier squarks are the decays into quarks plus charginos/neutralinos, decays into lighter squarks plus vector bosons and decays into lighter squarks plus Higgs bosons. All these squark decays have been extensively discussed at the tree-level[3, 4, 5]. The next generation of colliders, for example, CERN Large Hadron Collider (LHC) will be able to produce such kind of particles with masses up to 2.5 TeV[6], and a e^+e^- linear Collider (LC)[7] will be able to make precise measurements of their properties. Thus a more accurate calculation of the decay mechanisms beyond the tree-level is necessary to provide a solid basis for experimental analysis of observing these decays at the next generation of colliders. Up to now one-loop QCD and supersymmetric (SUSY) QCD corrections to the squark decays have been calculated[4, 8], and the Yukawa corrections to the squark decays into quarks plus charginos/neutralinos also were given in Ref.[9]. Very recently, a complete one-loop computation of the electroweak radiative corrections to the above processes has been presented by J. Guasch, W. Hollik and J. Solà[10]. But the electroweak radiative corrections to the heavier squark decays into lighter squarks plus vector bosons and decays into lighter squarks plus Higgs bosons have not been calculated yet, even Yukawa corrections to these processes. In this paper, we present the calculations of the Yukawa corrections of order $\mathcal{O}(\alpha_{ew}m_{t(b)}^2/m_W^2)$, $\mathcal{O}(\alpha_{ew}m_{t(b)}^3/m_W^3)$ and $\mathcal{O}(\alpha_{ew}m_{t(b)}^4/m_W^4)$ to the width of sbottom decay into lighter stop plus charged Higgs boson, i.e. the decay $\tilde{b}_i \rightarrow \tilde{t}_1 + H^-$, where \tilde{t}_1 is the lighter stop. These corrections are mainly induced by Yukawa couplings from Higgs-quark-quark couplings, Higgs-squark-squark couplings, Higgs-Higgs-squark-squark couplings, chargino(neutralino)-quark-squark couplings, and squark-squark-

squark-squark couplings.

Our results can be generalized straightforwardly to the decay $\tilde{t}_2 \rightarrow \tilde{t}_1 + (h^0, A^0)$. As for the heavier squark decays into lighter squarks plus vector bosons, the electroweak radiative corrections are simple because of the relatively less renormalization parameters involved.

2 Notation and tree-level result

In order to make this paper self-contained, we first summarize our notation and present the relevant interaction Lagrangians of the MSSM and the tree-level decay rates for $\tilde{b}_i \rightarrow \tilde{t}_1 + H^-$.

The current eigenstates \tilde{q}_L and \tilde{q}_R are related to the mass eigenstates \tilde{q}_1 and \tilde{q}_2 by:

$$\begin{pmatrix} \tilde{q}_1 \\ \tilde{q}_2 \end{pmatrix} = R^{\tilde{q}} \begin{pmatrix} \tilde{q}_L \\ \tilde{q}_R \end{pmatrix}, \quad R^{\tilde{q}} = \begin{pmatrix} \cos \theta_{\tilde{q}} & \sin \theta_{\tilde{q}} \\ -\sin \theta_{\tilde{q}} & \cos \theta_{\tilde{q}} \end{pmatrix} \quad (1)$$

with $0 \leq \theta_{\tilde{q}} < \pi$ by convention. Correspondingly, the mass eigenvalues $m_{\tilde{q}_1}$ and $m_{\tilde{q}_2}$ (with $m_{\tilde{q}_1} \leq m_{\tilde{q}_2}$) are given by

$$\begin{pmatrix} m_{\tilde{q}_1}^2 & 0 \\ 0 & m_{\tilde{q}_2}^2 \end{pmatrix} = R^{\tilde{q}} M_{\tilde{q}}^2 (R^{\tilde{q}})^\dagger, \quad M_{\tilde{q}}^2 = \begin{pmatrix} m_{\tilde{q}_L}^2 & a_q m_q \\ a_q m_q & m_{\tilde{q}_R}^2 \end{pmatrix} \quad (2)$$

with

$$m_{\tilde{q}_L}^2 = M_{\tilde{Q}}^2 + m_q^2 + m_Z^2 \cos 2\beta (I_{3L}^q - e_q \sin^2 \theta_W), \quad (3)$$

$$m_{\tilde{q}_R}^2 = M_{\{\tilde{U}, \tilde{D}\}}^2 + m_q^2 + m_Z^2 \cos 2\beta e_q \sin^2 \theta_W, \quad (4)$$

$$a_q = A_q - \mu \{\cot \beta, \tan \beta\} \quad (5)$$

for {up,down} type squarks. Here $M_{\tilde{q}}^2$ is the squark mass matrix. $M_{\tilde{Q}, \tilde{U}, \tilde{D}}$ and $A_{t,b}$ are soft supersymmetric breaking parameters and μ is the Higgs mixing parameter in the superpotential. I_{3L}^q and e_q are the third component of the weak isospin and the electric charge of the quark q , respectively.

Defining $H_k = (h^0, H^0, A^0, G^0, H^\pm, G^\pm)$ ($k=1\dots 6$), one can write the relevant lagrangian density in the $(\tilde{q}_1, \tilde{q}_2)$ basis as following form ($i, j=1,2$; α and β flavor indices)

$$\begin{aligned} \mathcal{L}_{\text{relevant}} = & H_k \bar{q}^\beta (a_k^\alpha P_L + b_k^\alpha P_R) q^\alpha + (G_k^{\tilde{\alpha}})_{ij} H_k \tilde{q}_j^{\beta*} \tilde{q}_i^\alpha + g \bar{q} (a_{ik}^{\tilde{q}} P_R + b_{ik}^{\tilde{q}}) \tilde{\chi}_k^0 \tilde{q}_i \\ & + g \bar{t} (l_{ik}^{\tilde{b}} P_R + k_{ik}^{\tilde{b}} P_L) \tilde{\chi}_k^+ \tilde{b}_i + g \bar{b} (l_{ik}^{\tilde{t}} P_R + k_{ik}^{\tilde{t}} P_L) \tilde{\chi}_k^{+c} \tilde{t}_i \\ & + (G_{5k}^{\tilde{\alpha}})_{ij} H^+ H_k \tilde{q}_j^{\beta*} \tilde{q}_i^\alpha + h.c., \end{aligned} \quad (6)$$

with

$$(G_k^{\tilde{\alpha}})_{ij} = [R^{\tilde{\alpha}} \hat{G}_k^{\tilde{\alpha}} (R^{\tilde{\beta}})^T]_{ij}, \quad (G_{5k}^{\tilde{\alpha}})_{ij} = [R^{\tilde{\alpha}} \hat{G}_{5k}^{\tilde{\alpha}} (R^{\tilde{\beta}})^T]_{ij} \quad (k = 1 \dots 6), \quad (7)$$

where $\hat{G}_k^{\tilde{\alpha}}$ and $\hat{G}_{5k}^{\tilde{\alpha}}$ are the couplings in the $(\tilde{q}_L, \tilde{q}_R)$ basis, and their explicit forms are shown in Appendix A. The notations a_k^{α} , b_k^{α} ($k=1 \dots 6$), and $a_{ik}^{\tilde{q}}$, $b_{ik}^{\tilde{q}}$ ($k=1 \dots 4$), and $l_{ik}^{\tilde{q}}$, $k_{ik}^{\tilde{q}}$ ($k=1,2$) used in Eq.(6) are defined also in Appendix A.

The tree-level amplitude of $\tilde{b}_i \rightarrow \tilde{t}_1 H^-$, as shown in Fig.1(a), is given by

$$M_i^{(0)} = \frac{ig}{\sqrt{2}m_W} [R^{\tilde{b}} \begin{pmatrix} m_b^2 \tan \beta + m_t^2 \cot \beta - m_W^2 \sin 2\beta & m_t(A_t \cot \beta + \mu) \\ m_b(A_b \tan \beta + \mu) & 2m_t m_b / \sin 2\beta \end{pmatrix} (R^{\tilde{t}})^T]_{i1}, \quad (8)$$

and the decay width is

$$\Gamma_i^{(0)} = \frac{|M_i^{(0)}|^2 \lambda^{1/2}(m_{\tilde{b}_i}^2, m_{\tilde{t}_1}^2, m_{H^-}^2)}{16\pi m_{\tilde{b}_i}^3} \quad (9)$$

with $\lambda(x, y, z) = (x - y - z)^2 - 4yz$.

3 Yukawa corrections

The Feynman diagrams contributing to the Yukawa corrections to $\tilde{b}_i \rightarrow \tilde{t}_1 H^-$ are shown in Figs.1(b)–(f) and Fig.2. We carried out the calculation in the t'Hooft-Feynman gauge and used the dimensional reduction, which preserves supersymmetry, for regularization of the ultraviolet divergences in the virtual loop corrections using the on-mass-shell renormalization scheme[11], in which the fine-structure constant α_{ew} and physical masses are chosen to be the renormalized parameters, and finite parts of the counterterms are fixed by the renormalization conditions. The coupling constant g is related to the input parameters e , m_W and m_Z via $g^2 = e^2/s_w^2$ and $s_w^2 = 1 - m_W^2/m_Z^2$. As for the renormalization of the parameters in the Higgs sector and the squark sector, it will be described below in detail.

The relevant renormalization constants are defined as

$$\begin{aligned} m_{W0}^2 &= m_W^2 + \delta m_W^2, & m_{Z0}^2 &= m_Z^2 + \delta m_Z^2, \\ m_{q0} &= m_q + \delta m_q, & m_{\tilde{q}_i0}^2 &= m_{\tilde{q}_i}^2 + \delta m_{\tilde{q}_i}^2, \\ A_{q0} &= A_q + \delta A_q, & \mu_0 &= \mu + \delta \mu, \end{aligned}$$

$$\begin{aligned}
\theta_{\tilde{q}0} &= \theta_{\tilde{q}} + \delta\theta_{\tilde{q}}, & \tan\beta_0 &= (1 + \delta Z_\beta) \tan\beta, \\
\tilde{q}_{i0} &= (1 + \delta Z_i^{\tilde{q}})^{1/2} + \delta Z_{ij}^{\tilde{q}} \tilde{q}_j, \\
H_0^- &= (1 + \delta Z_{H^-})^{1/2} H^- + \delta Z_{HG} G^-, \\
G_0^- &= (1 + \delta Z_{G^-})^{1/2} G^- + \delta Z_{GH} H^-
\end{aligned} \tag{10}$$

with $q = t, b$. Here we introduce the mixing of H^- and G^- [12], instead of the mixing of H^- and W^- [13]

$$\begin{aligned}
W_{\mu 0}^- &= (1 + \delta Z_{W^-})^{1/2} W_\mu^- + i Z_{WH} \partial_\mu H^-, \\
H_0^- &= (1 + \delta Z_{H^-})^{1/2} H^-,
\end{aligned} \tag{11}$$

due to the reason: the former can successfully cancel the divergences for the case we are considering, and the latter, however, is just right for the renormalization of the parameters β and α , and in the case that the particles interacting with the charged Higgs boson are the on-shell fermions (where a \not{p} arising from $\partial_\mu H^-$ and the vertex W^- -fermion-fermion is inserted between two on-shell fermions, and turned into the fermion masses by Dirac equations, which is therefore similar to the structure of the Yukawa coupling H^- -fermion-fermion).

Taking into account the Yukawa corrections, the renormalized amplitude for $\tilde{b}_i \rightarrow \tilde{t}_1 H^-$ is given by

$$M_i^{ren} = M_i^{(0)} + \delta M_i^{(v)} + \delta M_i^{(c)}, \tag{12}$$

where $\delta M_i^{(v)}$ and $\delta M_i^{(c)}$ are the vertex corrections and the counterterm, respectively.

The calculations of the vertex corrections from Fig.1(b)-1(f) result in

$$\begin{aligned}
\delta M_i^{(v)} &= \frac{i}{16\pi^2} \sum_{k=1}^6 \sum_j (G_{5k}^{\tilde{b}})_{ij} (G_k^{\tilde{q}})_{j1} B_0(p_{\tilde{t}_1}, m_{H_k}, m_{\tilde{q}_j}) \\
&+ \frac{i}{16\pi^2} \sum_{k=1}^6 \sum_j (G_k^{\tilde{b}})_{ij} (G_{5k}^{\tilde{q}})_{j1} B_0(p_{\tilde{b}_i}, m_{H_k}, m_{\tilde{q}_j}) \\
&- \frac{i}{16\pi^2} \sum_{k=1}^4 \sum_{j,l} (G_k^{\tilde{b}})_{ij} (G_5^{\tilde{b}})_{jl} (G_k^{\tilde{t}})_{l1} C_0(-p_{\tilde{b}_i}, p_{H^-}, m_{H_k}, m_{\tilde{b}_j}, m_{\tilde{t}_l}) \\
&+ \frac{ig^2}{8\pi^2} \sum_{k=1}^4 \{ [m_t m_b a_5^b + (m_{\tilde{b}_i}^2 - p_{\tilde{b}_i} \cdot p_{H^-}) b_5^b] m_{\tilde{\chi}_k^0} \tilde{b}_{ik}^{\tilde{b}} a_{1k}^{\tilde{t}*} C_0
\end{aligned}$$

$$\begin{aligned}
& +b_{ik}^{\tilde{b}}[m_b a_5^b b_{1k}^{\tilde{t}*}(p_{\tilde{b}_i} - p_{H^-}) + m_t b_5^b b_{1k}^{\tilde{t}*} p_{\tilde{b}_i} - m_{\tilde{\chi}_k^0} b_5^b a_{1k}^{\tilde{t}*}(2p_{\tilde{b}_i} - p_{H^-})]_{\mu}(-p_{\tilde{b}_i}^{\mu} C_{11} \\
& + p_{H^-}^{\mu} C_{12}) - (m_b a_5^b b_{1k}^{\tilde{t}*} + m_t b_5^b b_{1k}^{\tilde{t}*} - m_{\tilde{\chi}_k^0} b_5^b a_{1k}^{\tilde{t}*}) b_{ik}^{\tilde{b}}(m_{\tilde{b}_i}^2 C_{21} + m_{H^-}^2 C_{22} \\
& - 2p_{\tilde{b}_i} \cdot p_{H^-} C_{23} + g_{\mu}^{\mu} C_{24}) + (a \leftrightarrow b)\}(-p_{\tilde{b}_i}, p_{H^-}, m_{\tilde{\chi}_k^0}, m_b, m_t) \\
& - \frac{3i}{16\pi^2} \sum_{j,l} (h_b^2 R_{l2}^{\tilde{b}} R_{i2}^{\tilde{b}} R_{j1}^{\tilde{t}} R_{11}^{\tilde{t}} + h_t^2 R_{i1}^{\tilde{b}} R_{l1}^{\tilde{b}} R_{12}^{\tilde{t}} R_{j2}^{\tilde{t}})(G_5^{\tilde{b}})_{ij} B_0(p_{H^-}, m_{\tilde{b}_i}, m_{\tilde{t}_j}), \quad (13)
\end{aligned}$$

where B_0 and $C_{i(j)}$ are two- and three-point Feynman integrals[14], respectively, and $h_{t(b)}$ is the Yukawa coupling defined by

$$h_t = \frac{gm_t}{\sqrt{2}m_W \sin \beta}, \quad h_b = \frac{gm_b}{\sqrt{2}m_W \cos \beta}. \quad (14)$$

In the first line of $\delta M_i^{(v)}$, $q = t$ for $k = 1...4$ and $q = b$ for $k = 5, 6$, respectively, while in the second line, $q = b$ for $k = 1...4$ and $q = t$ for $k = 5, 6$, respectively.

The counterterm can be expressed as

$$\begin{aligned}
\delta M_i^{(c)} = & i(\delta\theta_{\tilde{b}} + \delta Z_{21}^{\tilde{b}})(G_5^{\tilde{b}})_{3-i,1} + i(\delta\theta_{\tilde{t}} + \delta Z_{21}^{\tilde{t}})(G_5^{\tilde{b}})_{i2} + i[R^{\tilde{b}}(\delta\hat{G}_5^{\tilde{b}})(R^{\tilde{t}})^T]_{i1} \\
& + \frac{i}{2}(\delta Z_i^{\tilde{b}} + \delta Z_1^{\tilde{t}} + \delta Z_{H^-})(G_5^{\tilde{b}})_{i1} + i\delta Z_{GH}(G_6^{\tilde{b}})_{i1} \quad (15)
\end{aligned}$$

with

$$\begin{aligned}
(\delta\hat{G}_5^{\tilde{b}})_{11} = & \frac{g}{\sqrt{2}m_W}[(\frac{\delta g}{g} - \frac{1}{2}\frac{\delta m_W^2}{m_W^2})(m_b^2 \tan \beta + m_t^2 \cot \beta) + 2m_b \tan \beta \delta m_b \\
& + 2m_t \cot \beta \delta m_t + m_b^2 \delta \tan \beta + m_t^2 \delta \cot \beta], \quad (16)
\end{aligned}$$

$$\begin{aligned}
(\delta\hat{G}_5^{\tilde{b}})_{12} = & \frac{g}{\sqrt{2}m_W}[(\frac{\delta g}{g} - \frac{1}{2}\frac{\delta m_W^2}{m_W^2} + \frac{\delta m_t}{m_t})m_t(A_t \cot \beta + \mu) + m_t(\delta A_t \cot \beta \\
& + A_t \delta \cot \beta + \delta \mu)], \quad (17)
\end{aligned}$$

$$\begin{aligned}
(\delta\hat{G}_5^{\tilde{b}})_{21} = & \frac{g}{\sqrt{2}m_W}[(\frac{\delta g}{g} - \frac{1}{2}\frac{\delta m_W^2}{m_W^2} + \frac{\delta m_b}{m_b})m_b(A_b \tan \beta + \mu) + m_b(\delta A_b \tan \beta \\
& + A_b \delta \tan \beta + \delta \mu)], \quad (18)
\end{aligned}$$

$$(\delta\hat{G}_5^{\tilde{b}})_{22} = \frac{2gm_b m_t}{\sqrt{2}m_W \sin 2\beta}(\frac{\delta g}{g} - \frac{1}{2}\frac{\delta m_W^2}{m_W^2} + \frac{\delta m_b}{m_b} + \frac{\delta m_t}{m_t} - \cos 2\beta \delta Z_{\beta}). \quad (19)$$

Here we consider only the corrections to the Yukawa couplings. The explicit expressions of some renormalization constants calculated from the self-energy diagrams in Fig.2 are given in Appendix B, and other renormalization constants are fixed as follows.

For δZ_{GH} , using the approach discussed in the two-Higgs doublet model (2HDM) in [12], we derived below its expression in the MSSM, where the version of the Higgs potential

is different from one of Ref. [12]. First, the one-loop renormalized two-point function is given by

$$i\Gamma_{GH}(p^2) = i(p^2 - m_{H^-}^2)\delta Z_{HG} + ip^2\delta Z_{GH} - iT_{GH} + i\Sigma_{GH}(p^2), \quad (20)$$

where T_{GH} is the tadpole function, which is given by

$$T_{GH} = \frac{g}{2m_W}[T_{H_2}\sin(\alpha - \beta) + T_{H_1}\cos(\alpha - \beta)]. \quad (21)$$

Next from the on-shell renormalization condition, we obtained

$$\delta Z_{GH} = \frac{1}{m_{H^-}^2}[T_{GH} - \Sigma_{GH}(m_{H^-}^2)]. \quad (22)$$

The explicit expressions of Σ_{GH} and the tadpole counterterms T_{H_k} ($k = 1, 2$) are given in Appendix B.

For the renormalization of the parameter β , following the analysis of Ref.[13], we fixed the renormalization constant by the requirement that the on-mass-shell $H^+\bar{\tau}\nu_\tau$ coupling remain the same form as in Eq.(3) of Ref.[13] to all orders of perturbation theory. However, with introducing the mixing of H^- and G^- instead of H^- and W^- , the expression of δZ_β is then changed to

$$\delta Z_\beta = \frac{1}{2}\frac{\delta m_W^2}{m_W^2} - \frac{1}{2}\frac{\delta m_Z^2}{m_Z^2} + \frac{1}{2}\frac{\delta m_Z^2 - \delta m_W^2}{m_Z^2 - m_W^2} - \frac{1}{2}\delta Z_{H^+} + \cot\beta\delta Z_{GH}. \quad (23)$$

For the counterterm of squark mixing angle $\theta_{\tilde{q}}$, using the same renormalized scheme as Ref.[9], one has

$$\delta\theta_{\tilde{q}} = \frac{\text{Re}[\Sigma_{12}^{\tilde{q}}(m_{\tilde{q}_1}^2) + \Sigma_{12}^{\tilde{q}}(m_{\tilde{q}_2}^2)]}{2(m_{\tilde{q}_1}^2 - m_{\tilde{q}_2}^2)}. \quad (24)$$

For the renormalization of soft SUSY-breaking parameter A_q , we fixed its counterterm by keeping the tree-level relation of A_q , $m_{\tilde{q}_i}$ and $\theta_{\tilde{q}}$ [15], and get the expression as following:

$$\begin{aligned} \delta A_q = & \frac{m_{\tilde{q}_1}^2 - m_{\tilde{q}_2}^2}{2m_q}(2\cos 2\theta_{\tilde{q}}\delta\theta_{\tilde{q}} - \sin 2\theta_{\tilde{q}}\frac{\delta m_q}{m_q}) + \frac{\sin 2\theta_{\tilde{q}}}{2m_q}(\delta m_{\tilde{q}_1}^2 - \delta m_{\tilde{q}_2}^2) \\ & + \{\cot\beta, \tan\beta\}\delta\mu + \delta\{\cot\beta, \tan\beta\}\mu. \end{aligned} \quad (25)$$

As for the parameter μ , there are several schemes[10, 16, 17] to fix its counterterm, and here we use the on-shell renormalization scheme in Ref.[17], which gives

$$\delta\mu = \sum_{k=1}^2[m_{\tilde{\chi}_k^+}(\delta U_{k2}V_{k2} + U_{k2}\delta V_{k2}) + \delta m_{\tilde{\chi}_k^+}U_{k2}V_{k2}], \quad (26)$$

where (U, V) are the two 2×2 matrices diagonalizing the chargino mass matrix, and their counterterms $(\delta U, \delta V)$ are given by

$$\delta U = \frac{1}{4}(\delta Z_R - \delta Z_R^T)U, \quad (27)$$

$$\delta V = \frac{1}{4}(\delta Z_L - \delta Z_L^T)V. \quad (28)$$

The mass shifts $\delta m_{\tilde{\chi}_k^+}$ and the off-diagonal wave function renormalization constants $\delta Z_{R(L)}$ can be written as

$$\delta m_{\tilde{\chi}_k^+} = \frac{1}{2}\text{Re}[m_{\tilde{\chi}_k^+}(\Pi_{kk}^L(m_{\tilde{\chi}_k^+}^2) + \Pi_{kk}^R(m_{\tilde{\chi}_k^+}^2)) + \Pi_{kk}^{S,L}(m_{\tilde{\chi}_k^+}^2) + \Pi_{kk}^{S,R}(m_{\tilde{\chi}_k^+}^2)], \quad (29)$$

$$(\delta Z_R)_{ij} = \frac{2}{m_{\tilde{\chi}_i^+}^2 - m_{\tilde{\chi}_j^+}^2}\text{Re}[\Pi_{ij}^R(m_{\tilde{\chi}_j^+}^2)m_{\tilde{\chi}_j^+}^2 + \Pi_{ij}^L(m_{\tilde{\chi}_j^+}^2)m_{\tilde{\chi}_i^+}m_{\tilde{\chi}_j^+} + \Pi_{ij}^{S,R}(m_{\tilde{\chi}_j^+}^2)m_{\tilde{\chi}_i^+} + \Pi_{ij}^{S,L}(m_{\tilde{\chi}_j^+}^2)m_{\tilde{\chi}_j^+}], \quad (30)$$

$$(\delta Z_L)_{ij} = (\delta Z_R)_{ij} \quad (L \leftrightarrow R). \quad (31)$$

The explicit expressions of the chargino self-energy matrices $\Pi^{L(R)}$ and $\Pi^{S,L(R)}$ are given in Appendix B.

Finally, the renormalized decay width is then given by

$$\Gamma_i = \Gamma_i^{(0)} + \delta\Gamma_i^{(v)} + \delta\Gamma_i^{(c)} \quad (32)$$

with

$$\delta\Gamma_i^{(a)} = \frac{\lambda^{1/2}(m_{b_i}^2, m_{t_1}^2, m_{H^-}^2)}{8\pi m_{b_i}^3}\text{Re}\{M_i^{(0)*}\delta M_i^{(a)}\} \quad (a = v, c). \quad (33)$$

4 Numerical results and conclusion

In the following we present some numerical results for the Yukawa corrections to sbottom decay into lighter stop plus charged Higgs boson. In our numerical calculations the SM parameters were taken to be $\alpha_{ew}(m_Z) = 1/128.8$, $m_W = 80.375\text{GeV}$, $m_Z = 91.1867\text{GeV}$ [18] and $m_t = 175.6\text{GeV}$. In order to improve the convergence of the perturbation expansion, especially for large $\tan\beta$, we take the running mass $m_b(Q)$ evaluated by the next-to-leading order formula[19]

$$m_b(Q) = U_6(Q, m_t)U_5(m_t, m_b)m_b(m_b), \quad (34)$$

where we have assumed that there are no other colored particles with masses between scale Q and m_t , and $m_b(m_b) = 4.25\text{GeV}$ [20]. The evolution factor U_f is

$$U_f(Q_2, Q_1) = \left(\frac{\alpha_s(Q_2)}{\alpha_s(Q_1)}\right)^{d^{(f)}} \left[1 + \frac{\alpha_s(Q_1) - \alpha_s(Q_2)}{4\pi} J^{(f)}\right],$$

$$d^{(f)} = \frac{12}{33 - 2f}, \quad J^{(f)} = -\frac{8982 - 504f + 40f^2}{3(33 - 2f)^2}, \quad (35)$$

where $\alpha_s(Q)$ is given by the solutions of the two-loop renormalization group equations[21]. When $Q = 400\text{GeV}$, the running mass $m_b(Q) \sim 2.5\text{GeV}$. In addition, we also improved the perturbation calculations by the following replacement in the tree-level couplings[19]

$$m_b(Q) \rightarrow \frac{m_b(Q)}{1 + \Delta m_b(M_{SUSY})} \quad (36)$$

where

$$\begin{aligned} \Delta m_b = & \frac{2\alpha_s}{3\pi} M_{\tilde{g}} \mu \tan \beta I(m_{\tilde{b}_1}, m_{\tilde{b}_2}, M_{\tilde{g}}) + \frac{h_t^2}{16\pi^2} \mu A_t \tan \beta I(m_{\tilde{t}_1}, m_{\tilde{t}_2}, \mu) \\ & - \frac{g^2}{16\pi^2} \mu M_2 \tan \beta [\cos^2 \theta_{\tilde{t}} I(m_{\tilde{t}_1}, M_2, \mu) + \sin^2 \theta_{\tilde{t}} I(m_{\tilde{t}_2}, M_2, \mu) \\ & + \frac{1}{2} \cos^2 \theta_{\tilde{b}} I(m_{\tilde{b}_1}, M_2, \mu) + \frac{1}{2} \sin^2 \theta_{\tilde{b}} I(m_{\tilde{b}_2}, M_2, \mu)] \end{aligned} \quad (37)$$

with

$$I(a, b, c) = \frac{1}{(a^2 - b^2)(b^2 - c^2)(a^2 - c^2)} (a^2 b^2 \log \frac{a^2}{b^2} + b^2 c^2 \log \frac{b^2}{c^2} + c^2 a^2 \log \frac{c^2}{a^2}). \quad (38)$$

The two-loop leading-log relations[22] of the neutral Higgs boson masses and mixing angles in the MSSM were used. For m_{H^+} the tree-level formula was used. Other MSSM parameters were determined as follows:

(i) For the parameters M_1 , M_2 and μ in the chargino and neutralino matrix, we take M_2 and μ as the input parameters, and then use the relation $M_1 = (5/3)(g'^2/g^2)M_2 \simeq 0.5M_2$ [2, 23] to determine M_1 . The gluino mass $M_{\tilde{g}}$ in Eq.(37) was related to M_2 by $M_{\tilde{g}} = (\alpha_s(M_{\tilde{g}})/\alpha_2)M_2$ [5].

(ii) For the parameters $m_{\tilde{Q}, \tilde{U}, \tilde{D}}^2$ and $A_{t,b}$ in squark mass matrices, we assumed $M_{\tilde{Q}} = M_{\tilde{U}} = M_{\tilde{D}}$ and $A_t = A_b$ to simplify the calculations.

Some typical numerical results of the tree-level decay widths and the Yukawa corrections are given in Fig.3-9.

Fig.3 and Fig.4 show the $m_{\tilde{t}_1}$ dependence of the results of \tilde{b}_1 and \tilde{b}_2 decays, respectively. Here we take $m_{A^0} = 150\text{GeV}$, $\mu = M_2 = 400\text{GeV}$ and $A_t = A_b = 1\text{TeV}$. The leading terms of the tree level amplitude are given by

$$M_i^{(0)} \sim \frac{ig}{\sqrt{2}m_W} [m_t(A_t \cot \beta + \mu) R_{i1}^{\tilde{b}} R_{12}^{\tilde{t}} + m_b(A_b \tan \beta + \mu) R_{i2}^{\tilde{b}} R_{11}^{\tilde{t}}], \quad (39)$$

where $\cos \theta_{\tilde{b}} \sim (0.54, 0.67, 0.70)$ and $\cos \theta_{\tilde{t}} \sim (-0.71, -0.71, -0.71)$ for $\tan \beta = (4, 10, 30)$, respectively. In the case of $i = 1$, two terms in Eq.(39) have opposite signs, and their magnitudes get close with the increasing $\tan \beta$ and thus cancel to large extent for large $\tan \beta$. Therefore, the tree level decay widths have the feature of $\Gamma_0(\tan \beta = 4) > \Gamma_0(\tan \beta = 10) > \Gamma_0(\tan \beta = 30)$ in the most of parameter range, as shown in Fig.3(a). In the case of $i = 2$, for $\tan \beta = 4, 10$ and 30 two terms in Eq.(39) have the same signs, so Γ_0 is larger than the one of the case of $i = 1$. From Fig.3(b) and Fig.4(b) one can see that the relative corrections are sensitive to the value of $\tan \beta$. For $\tan \beta = 30$, the magnitudes of the corrections can exceed 10% when $m_{\tilde{t}_1} > 160\text{GeV}$ for \tilde{b}_1 decay and $m_{\tilde{t}_1} > 260\text{GeV}$ for \tilde{b}_2 decay. Especially in the case of \tilde{b}_1 decay it even can reach 40%, which is due to the fact that the corresponding tree-level decay width already becomes very small. There are the dips at $m_{\tilde{t}_1} = 311\text{GeV}$ and 390GeV on the solid line in Fig.4(b), which come from the singularities at the threshold points $m_{\tilde{b}_2} = m_{\tilde{\chi}_1^+} + m_t$ and $m_{\tilde{b}_1} = m_{\tilde{\chi}_1^+} + m_t$, respectively. However, for $\tan \beta = 4$ and 10 , the corrections of two sbottom decays are always small and range from -5% to 5% . In general, for low $\tan \beta$ the top quark contribution is enhanced while for high $\tan \beta$ the bottom quark contribution become large, and for medium $\tan \beta$, there are not any enhanced effects from Yukawa couplings. So the corrections for $\tan \beta = 4$ are generally larger than those for $\tan \beta = 10$, as shown in Fig.3(b) and Fig.4(b).

Fig.5 (Fig.6) gives the tree-level decay width and the Yukawa corrections as the functions of m_{H^-} in the case of \tilde{b}_1 decay (\tilde{b}_2 decay). We assumed $m_{\tilde{t}_1} = 170\text{GeV}$, $\mu = M_2 = 400\text{GeV}$ and $A_t = A_b = 1\text{TeV}$. The features of the tree level decay widths in Fig.5(a) and Fig.6(a) are similar to Fig.3(a) and Fig.4(a), respectively. From Fig.5(b) and Fig.6(b) we can see that the relative corrections decrease or increase the decay widths depending on $\tan \beta$. Fig.5(b) shows that the corrections for $\tan \beta = 4$ are always positive and range between 6% and 3% . For $\tan \beta = 10$ the corrections are negligibly small. For high $\tan \beta (= 30)$ the

corrections exceed 10% when $m_{H^-} < 180\text{GeV}$. There is a dip at $m_{H^-} \sim 178\text{GeV}$ on the solid curve due to the singularity of the charged Higgs boson wave function renormalization constant at the threshold point $m_{H^-} = m_t + m_b$. Fig.6(b) shows that the corrections are a few percent for $\tan\beta = 4, 10$ and 30 . There are a dip and a peak on the solid curve, which arise from the singularities at the threshold points $m_{\tilde{b}_2} = m_{\tilde{b}_1} + m_{A^0}$ and $m_{H^-} = m_t + m_b$, respectively.

In Fig.7 and Fig.8 we present the tree level decay widths and the Yukawa corrections as the functions of μ in the case of $\tilde{b}_1 \rightarrow \tilde{t}_1 + H^-$ and $\tilde{b}_2 \rightarrow \tilde{t}_1 + H^-$, respectively, assuming $m_{\tilde{t}_1} = 170\text{GeV}$, $M_2 = 400\text{GeV}$, $A_t = A_b = 1\text{TeV}$ and $m_{A^0} = 150\text{GeV}$. When μ takes some values, the tree level decay widths are getting very small ($< 10^{-3}\text{GeV}$), as shown in Fig.7(a) and Fig.8(a), and the corrections near the above values do not have a physical meaning. So we cut off the corrections, since perturbation theory breaks down there. From Fig.7(a) (Fig.8(a)) we can see that there is a high peak (a deep dip) for $\tan\beta = 30$ and $\mu \sim 30\text{GeV}$. This is due to the fact that when $\tan\beta = 30$ and $\mu \sim 30\text{GeV}$ the second term in Eq.(39) is enhanced (suppressed) greatly for $\sin\theta_{\tilde{b}} \sim 1$ ($\cos\theta_{\tilde{b}} \sim 0$) as a result of the off-diagonal elements of $M_{\tilde{b}}^2$ in Eq.(2) approaching to zero. Fig.7(b) and Fig.8(b) show that the Yukawa corrections depend on μ strongly. Especially, in the region of Γ_0 getting very small, the corrections get the rapid variations between the positive and negative values with the changes of the sign of the tree level amplitude. In general, when the tree-level decay widths for $\tan\beta = 4$ and 10 are not close to zero, the corrections are always small. Comparing Fig.7(b) with Fig.8(b), we can find that the Yukawa corrections for $\tan\beta = 30$ are more significant for \tilde{b}_1 decay than for \tilde{b}_2 decay.

Finally, in Fig.9 we show the Yukawa corrections as a function of $\tan\beta$ in three ways of perturbative expansion: (i) the strict on-shell scheme (the dashed line), where the bottom quark pole mass 4.7GeV was used, (ii) the QCD-improved scheme (the dotted line), in which only QCD running bottom quark mass $m_b(Q)$ in Eq.(34) was used, and (iii) the improved scheme (the solid line), in which the replacement Eq.(36) was used. Here we assumed $m_{\tilde{t}_1} = 170\text{GeV}$, $\mu = M_2 = 400\text{GeV}$, $A_t = A_b = 1\text{TeV}$ and $m_{A^0} = 150\text{GeV}$. One can see that the three ways all give small corrections ($|\delta\Gamma/\Gamma_0| < 5\%$) for $\tan\beta (< 15)$.

However, the magnitude of the corrections in the case (i) increases rapidly for $\tan\beta > 15$, and when $\tan\beta > 33$ the corrections will result in the physically meaningless negative width. But the convergences in the cases (ii) and (iii) are much better, and especially in the case (iii) the magnitude of the corrections still is less than 40% for high values of $\tan\beta$ ($=40$).

In conclusion, we have calculated the Yukawa corrections to the width of sbottom decay into lighter stop plus charged Higgs boson in MSSM. These corrections depend on the masses of charged Higgs boson and lighter stop, and the parameters $\tan\beta$ and μ . For favorable parameter values, the corrections decrease or increase the decay widths significantly. Especially for high values of $\tan\beta(=30)$ the corrections exceed at least 10% for both \tilde{b}_1 and \tilde{b}_2 decay. But for low values of $\tan\beta(=4,10)$ the corrections are small and the magnitudes are less than 10%. The numerical calculations also show that using the running bottom quark mass which includes the QCD effects and resums all high order $\tan\beta$ -enhanced effects, as given in Ref.[19], can improve much the convergence of the perturbation expansion.

Acknowledgements

We thank Ya Sheng Yang for giving help in numerical calculations. This work was supported in part by the National Natural Science Foundation of China, the Doctoral Program Foundation of Higher Education of China, and a grant from the State Commission of Science and Technology of China.

Appendix A

The following couplings are given in order $O(h_t, h_b)$.

1. squark – squark – Higgs boson

(a) squark – squark – h^0

$$\hat{G}_1^{\tilde{q}\tilde{q}} = \begin{pmatrix} -\sqrt{2}m_q h_q \begin{Bmatrix} c_\alpha \\ -s_\alpha \end{Bmatrix} & -\frac{1}{\sqrt{2}}h_q(A_q \begin{Bmatrix} c_\alpha \\ -s_\alpha \end{Bmatrix} + \mu \begin{Bmatrix} s_\alpha \\ c_\alpha \end{Bmatrix}) \\ -\frac{1}{\sqrt{2}}h_q(A_q \begin{Bmatrix} c_\alpha \\ -s_\alpha \end{Bmatrix} + \mu \begin{Bmatrix} s_\alpha \\ c_\alpha \end{Bmatrix}) & -\sqrt{2}m_q h_q \begin{Bmatrix} c_\alpha \\ -s_\alpha \end{Bmatrix} \end{pmatrix} \quad (40)$$

for $\left\{ \begin{array}{c} \text{up} \\ \text{down} \end{array} \right\}$ type squarks, respectively. We use the abbreviations $s_\alpha = \sin \alpha$, $c_\alpha = \cos \alpha$. α is the mixing angle in the CP even neutral Higgs boson sector.

(b) squark – squark – H^0

$$\hat{G}_2^{\tilde{q}} = \begin{pmatrix} -\sqrt{2}m_q h_q \begin{Bmatrix} s_\alpha \\ c_\alpha \end{Bmatrix} & -\frac{1}{\sqrt{2}}h_q(A_q \begin{Bmatrix} s_\alpha \\ c_\alpha \end{Bmatrix} - \mu \begin{Bmatrix} c_\alpha \\ s_\alpha \end{Bmatrix}) \\ -\frac{1}{\sqrt{2}}h_q(A_q \begin{Bmatrix} s_\alpha \\ c_\alpha \end{Bmatrix} - \mu \begin{Bmatrix} c_\alpha \\ s_\alpha \end{Bmatrix}) & -\sqrt{2}m_q h_q \begin{Bmatrix} s_\alpha \\ c_\alpha \end{Bmatrix} \end{pmatrix} \quad (41)$$

(c) squark – squark – A^0

$$\hat{G}_3^{\tilde{q}} = i \frac{gm_q}{2m_W} \begin{pmatrix} 0 & -A_q \begin{Bmatrix} \cot \beta \\ \tan \beta \end{Bmatrix} - \mu \\ A_q \begin{Bmatrix} \cot \beta \\ \tan \beta \end{Bmatrix} + \mu & 0 \end{pmatrix} \quad (42)$$

(d) squark – squark – G^0

$$\hat{G}_4^{\tilde{q}} = i \frac{gm_q}{2m_W} \begin{pmatrix} 0 & -A_q + \mu \begin{Bmatrix} \cot \beta \\ \tan \beta \end{Bmatrix} \\ A_q - \mu \begin{Bmatrix} \cot \beta \\ \tan \beta \end{Bmatrix} & 0 \end{pmatrix} \quad (43)$$

(e) squark – squark – H^\pm

$$\hat{G}_5^{\tilde{b}} = (\hat{G}_5^{\tilde{t}})^T = \frac{g}{\sqrt{2}m_W} \begin{pmatrix} m_b^2 \tan \beta + m_t^2 \cot \beta & m_t(A_t \cot \beta + \mu) \\ m_b(A_b \tan \beta + \mu) & 2m_t m_b / \sin 2\beta \end{pmatrix} \quad (44)$$

(f) squark – squark – G^\pm

$$\hat{G}_6^{\tilde{b}} = (\hat{G}_6^{\tilde{t}})^T = \frac{g}{\sqrt{2}m_W} \begin{pmatrix} m_t^2 - m_b^2 & m_t(A_t - \mu \cot \beta) \\ m_b(\mu \tan \beta - A_b) & 0 \end{pmatrix} \quad (45)$$

2. quark – quark – Higgs boson

$$a_k^q = \left(\frac{1}{\sqrt{2}}h_q \begin{Bmatrix} -c_\alpha \\ s_\alpha \end{Bmatrix}, -\frac{1}{\sqrt{2}}h_q \begin{Bmatrix} s_\alpha \\ c_\alpha \end{Bmatrix}, -\frac{i}{\sqrt{2}}h_q \begin{Bmatrix} \cos \beta \\ \sin \beta \end{Bmatrix}, \frac{ig}{2m_W} \begin{Bmatrix} -m_t \\ m_b \end{Bmatrix}, \right. \\ \left. \begin{Bmatrix} h_b \sin \beta \\ h_t \cos \beta \end{Bmatrix}, \frac{g}{\sqrt{2}m_W} \begin{Bmatrix} -m_b \\ m_t \end{Bmatrix} \right) \quad (46)$$

$$b_k^q = \left(\frac{1}{\sqrt{2}}h_q \begin{Bmatrix} -c_\alpha \\ s_\alpha \end{Bmatrix}, -\frac{1}{\sqrt{2}}h_q \begin{Bmatrix} s_\alpha \\ c_\alpha \end{Bmatrix}, -\frac{i}{\sqrt{2}}h_q \begin{Bmatrix} \cos \beta \\ \sin \beta \end{Bmatrix}, \frac{ig}{2m_W} \begin{Bmatrix} m_t \\ -m_b \end{Bmatrix}, \right. \\ \left. h_q \begin{Bmatrix} \cos \beta \\ h_t \sin \beta \end{Bmatrix}, \frac{g}{\sqrt{2}m_W} \begin{Bmatrix} m_t \\ -m_b \end{Bmatrix} \right) \quad (47)$$

3. quark – squark – neutralino

$$a_{ik}^{\tilde{q}} = -R_{i2}^{\tilde{q}} Y_q \left\{ \begin{array}{c} N_{k4} \\ N_{k3} \end{array} \right\}, \quad b_{ik}^{\tilde{q}} = -R_{i1}^{\tilde{q}} Y_q \left\{ \begin{array}{c} N_{k4}^* \\ N_{k3}^* \end{array} \right\} \quad (48)$$

Here N is the 4×4 unitary matrix diagonalizing the neutral gaugino-higgsino mass matrix [2, 23], and the Yukawa factor $Y_q = h_q/g$.

4. quark – squark – chargino

$$l_{ik}^{\tilde{q}} = R_{i2}^{\tilde{q}} Y_q \left\{ \begin{array}{c} V_{k2} \\ U_{k2} \end{array} \right\}, \quad k_{ik}^{\tilde{q}} = R_{i1}^{\tilde{q}} \left\{ \begin{array}{c} Y_b U_{k2} \\ Y_t V_{k2} \end{array} \right\}. \quad (49)$$

Here U and V are the 2×2 unitary matrices diagonalizing the charged gaugino-higgsino mass matrix [2, 23].

5. squark – squark – Higgs boson – Higgs boson

(a) squark – squark – H^- – H_k ($k=1\dots 4$)

$$\hat{G}_{5k}^{\tilde{b}} = (\hat{G}_{5k}^{\tilde{t}})^T = \frac{g^2}{2\sqrt{2}m_W^2} \left(\begin{array}{cc} m_t^2 S_k + m_b^2 T_k & 0 \\ 0 & 2m_t m_b / \sin 2\beta V_k \end{array} \right) \quad (50)$$

with

$$S_k = (\cos \alpha \cos \beta / \sin^2 \beta, \quad \sin \alpha \cos \beta / \sin^2 \beta, \quad -i \cot^2 \beta, \quad i \cot \beta) \quad (51)$$

$$T_k = (-\sin \alpha \sin \beta / \cos^2 \beta, \quad \cos \alpha \sin \beta / \cos^2 \beta, \quad i \tan^2 \beta, \quad i \tan \beta) \quad (52)$$

$$V_k = (\sin(\beta - \alpha), \quad \cos(\beta - \alpha), \quad 0, \quad i) \quad (53)$$

(b) squark – squark – H^- – H^+

$$\hat{G}_{55}^{\tilde{q}} = \left(\begin{array}{cc} -\left\{ \begin{array}{c} h_b^2 \sin^2 \beta \\ h_t^2 \cos^2 \beta \end{array} \right\} & 0 \\ 0 & -h_q^2 \left\{ \begin{array}{c} \cos^2 \beta \\ \sin^2 \beta \end{array} \right\} \end{array} \right) \quad (54)$$

(c) squark – squark – H^- – G^+

$$\hat{G}_{56}^{\tilde{q}} = -\frac{g^2}{2m_W^2} \left(\begin{array}{cc} \left\{ \begin{array}{c} -m_b^2 \tan \beta \\ m_t^2 \cot \beta \end{array} \right\} & 0 \\ 0 & m_q^2 \left\{ \begin{array}{c} \cot \beta \\ -\tan \beta \end{array} \right\} \end{array} \right) \quad (55)$$

Appendix B

We define $q = t$ and b, q' the $SU(2)_L$ partner of q , and $q'' = q$ for $k = 1...4$ and $q'' = q'$ for $k = 5, 6$. Then we have

$$\begin{aligned}
\frac{\delta m_W^2}{m_W^2} &= \frac{g^2}{16\pi^2 m_W^2} [m_b^2 + m_t^2 - A_0(m_t^2) - A_0(m_b^2) - m_t^2 B_0 - (m_t^2 - m_b^2) B_1] \\
&\quad (m_W^2, m_b, m_t), \\
\frac{\delta m_Z^2}{m_Z^2} &= \frac{3g^2}{8\pi^2 m_W^2} \sum_{q=t,b} \left\{ \frac{1}{3} [(I_{3L}^q - e_q \sin^2 \theta_W)^2 + e_q^2 \sin^4 \theta_W] [2m_q^2 - 2A_0(m_q^2) - m_q^2 B_0] \right. \\
&\quad \left. - 2m_q^2 e_q \sin^2 \theta_W (I_{3L}^q - e_q \sin^2 \theta_W) B_0 \right\} (m_Z^2, m_q, m_q), \\
\delta Z_{H^-} &= \frac{3}{16\pi^2} \{ 2[(a_5^t b_5^b + b_5^t a_5^b)(m_{H^+}^2 G_1 + B_1 + m_b^2 G_0) + m_t m_b (a_5^t a_5^b + b_5^t b_5^b) G_0] \\
&\quad (m_{H^+}^2, m_b, m_t) - \sum_{j,l} (G_5^{\tilde{b}})_{jl} (G_5^{\tilde{t}})_{lj} G_0(m_{H^+}^2, m_{\tilde{b}_l}, m_{\tilde{t}_j}) \}, \\
T_{H_k} &= \frac{3}{16\pi^2} \sum_{q=t,b} \{ 2(a_k^q + b_k^q) m_q A_0(m_q^2) - \sum_j (G_k^{\tilde{q}})_{jj} A_0(m_{\tilde{q}_j}^2) \}, \\
\Sigma_{GH} &= -\frac{3}{16\pi^2} \{ 2[(a_5^t b_6^b + b_5^t a_6^b)(m_{H^+}^2 B_1 + A_0(m_t^2) + m_b^2 B_0) + m_t m_b (a_5^t a_6^b \\
&\quad + b_5^t b_6^b) B_0] (m_{H^+}^2, m_b, m_t) - \sum_{j,l} (G_5^{\tilde{t}})_{jl} (G_6^{\tilde{b}})_{lj} B_0(m_{H^+}^2, m_{\tilde{b}_l}, m_{\tilde{t}_j}) \\
&\quad + \sum_{q=t,b} \sum_j (G_{56}^{\tilde{q}})_{jj} A_0(m_{\tilde{q}_j}^2) \}, \\
\frac{\delta m_q}{m_q} &= \frac{1}{16\pi^2} \left\{ \sum_{k=1}^6 \left[\frac{m_{q''}}{m_q} a_k^q a_k^{q''} B_0 - \frac{1}{2} (a_k^q b_k^{q''} + b_k^q a_k^{q''}) B_1 \right] (m_q^2, m_{q''}, m_{H_k}) \right. \\
&\quad + g^2 \sum_{k=1}^4 \sum_j \left[\frac{m_{\tilde{\chi}_k^0}}{m_q} a_{jk}^{\tilde{q}} b_{jk}^{\tilde{q}*} B_0 - \frac{1}{2} (|a_{jk}^{\tilde{q}}|^2 + |b_{jk}^{\tilde{q}}|^2) B_1 \right] (m_q^2, m_{\tilde{\chi}_k^0}, m_{\tilde{q}_j}) \\
&\quad \left. + g^2 \sum_{k=1}^2 \sum_j \left[\frac{m_{\tilde{\chi}_k^+}}{m_q} l_{jk}^{\tilde{q}'} k_{jk}^{\tilde{q}'*} B_0 - \frac{1}{2} (|l_{jk}^{\tilde{q}'}|^2 + |k_{jk}^{\tilde{q}'}|^2) B_1 \right] (m_q^2, m_{\tilde{\chi}_k^+}, m_{\tilde{q}_j'}) \right\}, \\
\delta m_{\tilde{q}_i}^2 &= \frac{1}{16\pi^2} \left\{ \sum_{k=1}^6 \sum_j (G_k^{\tilde{q}})_{ij} (G_k^{\tilde{q}''})_{ji} B_0(m_{\tilde{q}_i}^2, m_{\tilde{q}_j''), m_{H_k}) - 2g^2 \sum_{k=1}^4 [(|a_{ik}^{\tilde{q}}|^2 + |b_{ik}^{\tilde{q}}|^2) \right. \\
&\quad \times (m_{\tilde{q}_i}^2 B_1 + A_0(m_{\tilde{\chi}_k^0}^2) + m_q^2 B_0) + 2m_q m_{\tilde{\chi}_k^0} \text{Re}(a_{ik}^{\tilde{q}} b_{ik}^{\tilde{q}*}) B_0] (m_{\tilde{q}_i}^2, m_q, m_{\tilde{\chi}_k^0}) \\
&\quad - 2g^2 \sum_{k=1}^2 [(|l_{ik}^{\tilde{q}}|^2 + |k_{ik}^{\tilde{q}}|^2) (m_{\tilde{q}_i}^2 B_1 + A_0(m_{\tilde{\chi}_k^+}^2) + m_{q'}^2 B_0) \\
&\quad \left. + 2m_{q'} m_{\tilde{\chi}_k^+} \text{Re}(l_{ik}^{\tilde{q}} k_{ik}^{\tilde{q}*}) B_0] (m_{\tilde{q}_i}^2, m_{q'}, m_{\tilde{\chi}_k^+}) \right\}, \\
\delta Z_{\tilde{q}_i} &= \frac{1}{16\pi^2} \left\{ - \sum_{k=1}^6 \sum_j (G_k^{\tilde{q}})_{ij} (G_k^{\tilde{q}''})_{ji} G_0(m_{\tilde{q}_i}^2, m_{\tilde{q}_j''), m_{H_k}) + 2g^2 \sum_{k=1}^4 [(|a_{ik}^{\tilde{q}}|^2 + |b_{ik}^{\tilde{q}}|^2) \right.
\end{aligned}$$

$$\begin{aligned}
& \times (B_1 + m_{\tilde{q}_i}^2 G_1 + m_q^2 G_0) + 2m_q m_{\tilde{\chi}_k^0} \text{Re}(a_{ik}^{\tilde{q}} b_{ik}^{\tilde{q}*}) G_0](m_{\tilde{q}_i}^2, m_q, m_{\tilde{\chi}_k^0}) \\
& + 2g^2 \sum_{k=1}^2 [(|l_{ik}^{\tilde{q}}|^2 + |k_{ik}^{\tilde{q}}|^2)(B_1 + m_{\tilde{q}_i}^2 G_1 + m_q^2 G_0) \\
& + 2m_{q'} m_{\tilde{\chi}_k^+} \text{Re}(l_{ik}^{\tilde{q}} k_{ik}^{\tilde{q}*}) G_0](m_{\tilde{q}_i}^2, m_{q'}, m_{\tilde{\chi}_k^+})\}, \\
\Sigma_{12}^{\tilde{q}}(p^2) &= \frac{1}{16\pi^2} \left\{ \sum_{k=1}^6 \sum_j (G_k^{\tilde{q}})_{1j} (G_k^{\tilde{q}''})_{j2} B_0(p^2, m_{\tilde{q}_j' }, m_{H_k}) - 2g^2 \sum_{k=1}^4 [(a_{1k}^{\tilde{q}} a_{2k}^{\tilde{q}*} + b_{1k}^{\tilde{q}} b_{2k}^{\tilde{q}*}) \right. \\
& \times (p^2 B_1 + A_0(m_{\tilde{\chi}_k^0}^2) + m_q^2 B_0) + m_q m_{\tilde{\chi}_k^0} (a_{1k}^{\tilde{q}} b_{2k}^{\tilde{q}*} + a_{2k}^{\tilde{q}*} b_{1k}^{\tilde{q}}) B_0](p^2, m_q, m_{\tilde{\chi}_k^0}) \\
& - 2g^2 \sum_{k=1}^2 [(l_{1k}^{\tilde{q}} l_{2k}^{\tilde{q}*} + k_{1k}^{\tilde{q}} k_{2k}^{\tilde{q}*}) (p^2 B_1 + A_0(m_{\tilde{\chi}_k^+}^2) + m_{q'}^2 B_0) \\
& \left. + m_{q'} m_{\tilde{\chi}_k^+} (l_{1k}^{\tilde{q}} k_{2k}^{\tilde{q}*} + l_{2k}^{\tilde{q}*} k_{1k}^{\tilde{q}}) B_0](p^2, m_{q'}, m_{\tilde{\chi}_k^+}) \right\}, \\
\delta\theta_{\tilde{q}} + \delta Z_{21}^{\tilde{q}} &= \frac{1}{2(m_{\tilde{q}_1}^2 - m_{\tilde{q}_2}^2)} [\Sigma_{12}^{\tilde{q}}(m_{\tilde{q}_2}^2) - \Sigma_{12}^{\tilde{q}}(m_{\tilde{q}_1}^2)], \\
\Pi_{ij}^L(p^2) &= -\frac{3}{16\pi^2} \sum_{k=1}^2 [l_{ki}^{\tilde{t}} l_{kj}^{\tilde{t}} B_1(p^2, m_b, m_{\tilde{t}_k}) + k_{ki}^{\tilde{b}} k_{kj}^{\tilde{b}} B_1(p^2, m_t, m_{\tilde{b}_k})], \\
\Pi_{ij}^R(p^2) &= -\frac{3}{16\pi^2} \sum_{k=1}^2 [k_{ki}^{\tilde{t}} k_{kj}^{\tilde{t}} B_1(p^2, m_b, m_{\tilde{t}_k}) + l_{ki}^{\tilde{b}} l_{kj}^{\tilde{b}} B_1(p^2, m_t, m_{\tilde{b}_k})], \\
\Pi_{ij}^{S,L}(p^2) &= \frac{3}{16\pi^2} \sum_{k=1}^2 [m_b k_{ki}^{\tilde{t}} l_{kj}^{\tilde{t}} B_0(p^2, m_b, m_{\tilde{t}_k}) + m_t l_{ki}^{\tilde{b}} k_{kj}^{\tilde{b}} B_0(p^2, m_t, m_{\tilde{b}_k})], \\
\Pi_{ij}^{S,R}(p^2) &= \frac{3}{16\pi^2} \sum_{k=1}^2 [m_b l_{ki}^{\tilde{t}} k_{kj}^{\tilde{t}} B_0(p^2, m_b, m_{\tilde{t}_k}) + m_t k_{ki}^{\tilde{b}} l_{kj}^{\tilde{b}} B_0(p^2, m_t, m_{\tilde{b}_k})].
\end{aligned}$$

Here A_0 and B_1 are one- and two-point Feynman integrals[14], respectively, and $G_i = \partial B_i / \partial p^2$.

References

- [1] H.P. Nilles, Phys. Rep. **110**, 1 (1984); A.B. Lahanas, D.V. Nanopoulos, Phys. Rep. **145**, 1 (1987); S. Ferrara, ed., *Supersymmetry*, vol. 1-2, North Holland/World Scientific, Singapore, 1987.
- [2] H.E. Haber and G.L. Kane, Phys. Rep. **117**, 75 (1985).
- [3] H. Baer, V. Barger, D. Karatas and X. Tata, Phys. Rev. D **36**, 96 (1987); K. Hikasa and M. Kobayashi, Phys. Rev. D **36**, 724 (1987); R.M. Barnett, J.F. Gunion and H.E. Haber, Phys. Rev. D **37**, 1892 (1988); H. Baer, X. Tata and J. Woodside, Phys. Rev.

- D **42**, 1568 (1990); K. Hikasa and M. Drees, Phys. Lett. B **252**, 127 (1990); A. Bartl, W. Majerotto, B. Mösslacher and N. Oshimo, Z. Phys. C **52**, 477 (1991); A. Bartl, W. Majerotto and W. Porod, Z. Phys. C **64**, 499 (1994); C **68**, 518(E) (1995).
- [4] A. Bartl, H. Eberl, K. Hidaka, S. Kraml, T. Kon, W. Majerotto, W. Porod and Y. Yamada, Phys. Lett. B **435** 118 (1998).
- [5] K. Hidaka and A. Bartl, Phys. Lett. B **501**, 78 (2001).
- [6] Atlas Collaboration, *Atlas Technical Design Report* CERN/LHCC/99-14/15; CMS Collaboration, *CMS Technical Proposal* CERN/LHCC/94-38; F. Gianotti, proceedings of the *IVth International Symposium on Radiative Corrections (RADCOR 98)*, p. 270, World Scientific 1999, ed. J. Solà.
- [7] D.J. Miller, proceedings of the *IVth International Symposium on Radiative Corrections (RADCOR 98)*, p. 289, World Scientific 1999, ed. J. Solà, hep-ex/9901039.
- [8] S. Kraml, H. Eberl, A. Bartl, W. Majerotto and W. Porod, Phys. Lett. B **386**, 175 (1996); A. Djouadi, W. Hollik and C. Jünger, Phys. Rev. D **55**, 6975 (1997); A. Bartl, H. Eberl, K. Hidaka, S. Kraml, W. Majerotto, W. Porod and Y. Yamada, hep-ph/9806299.
- [9] J. Guasch, W. Hollik and J. Solà, Phys. Lett. B **437**, 88 (1998).
- [10] J. Guasch, W. Hollik and J. Solà, hep-ph/0101086.
- [11] S. Sirlin, Phys. Rev. D **22**, 971 (1980); W.J. Marciano and A. Sirlin, *ibid.* **22**, 2695 (1980); **31**, 213(E) (1985); A. Sirlin and W.J. Marciano, Nucl. Phys. **B189**, 442 (1981); K.I. Aoki et.al., Prog. Theor. Phys. Suppl. **73**, 1 (1982).
- [12] R. Santos and A. Barroso, Phys. Rev. D **56**, 5366 (1997).
- [13] A. Mendez and A. Pomarol, Phys. Lett. B **279**, 98 (1992).

- [14] G 't Hooft and M. Veltman, Nucl. Phys. **B44**, 189 (1972); G. Passarino and M. Veltman, Nucl. Phys. **B160**, 151 (1979); A. Axelrod, *ibid.* **B209**, 349 (1982); M. Clements *et al.*, Phys. Rev. D **27**, 570 (1983).
- [15] A. Bartl, H. Eberl, K. Hidaka, T. Kon, W. Majerotto and Y. Yamada, Phys. Lett. B **402**, 303 (1997).
- [16] D. Pierce, A. Papadopoulos, Phys. Rev. D **50** 565 (1994).
- [17] H. Eberl, M. Kincel, W. Majerotto and Y. Yamada, hep-ph/0104109.
- [18] Particle Data Group, C.Caso *et al.*, Eur. Phys. J. C **3**, 1 (1998).
- [19] M. Carena, D. Garcia, U. Nierste, C.E.M. Wagner, Nucl. Phys. **B577**, 88 (2000).
- [20] M. Beneke and A. Signer, Phys. Lett. B **471**, 233 (1999); A.H. Hoang, Phys. Rev. D **61**, 034005 (2000).
- [21] S.G. Gorishny, A.L. Kataev, S.A. Larin, and L.R. Surguladze, Mod. Phys. Lett. A **5**, 2703 (1990); Phys. Rev. D **43**, 1633 (1991); A. Djouadi, M. Spira, and P.M. Zerwas, Z. Phys. C **70**, 427 (1996); A. Djouadi, J. Kalinowski, and M. Spira, Comput. Phys. Commun. **108**, 56 (1998); M. Spira, Fortschr. Phys. **46**, 203 (1998).
- [22] M. Carena, M. Quirós, C.E.M. Wagner, Nucl. Phys. **B461**, 407 (1996).
- [23] P. Nath, R. Arnowitt and A. Chamseddine, Applied $N = 1$ Supergravity, ICTP series in Theoretical Physics (World Scientific, 1984); J.F. Gunion and H.E. Haber, Nucl. Phys. **B272**, 1 (1986); L.E. Ibáñez and G.G. Ross, hep-ph/9204201, in: Perspectives on Higgs Physics, ed. G.L. Kane (World Scientific, 1993).

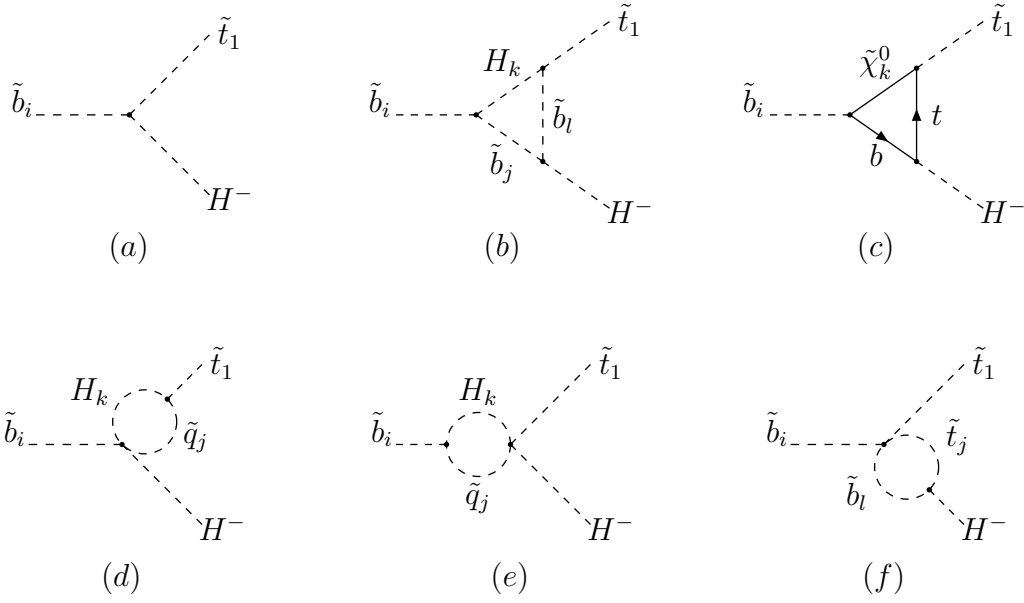


Figure 1: Feynman diagrams contributing to supersymmetric electroweak corrections to $\tilde{b}_i \rightarrow \tilde{t}_1 H^-$: (a) is tree level diagram; (b) – (f) are one-loop vertex corrections. In diagram (b) the subscript k of H_k can take from 1 to 4. In diagram (d) $q = t$ for $k = 1 \dots 4$ and $q = b$ for $k = 5, 6$. In diagram (e) $q = b$ for $k = 1 \dots 4$ and $q = t$ for $k = 5, 6$.

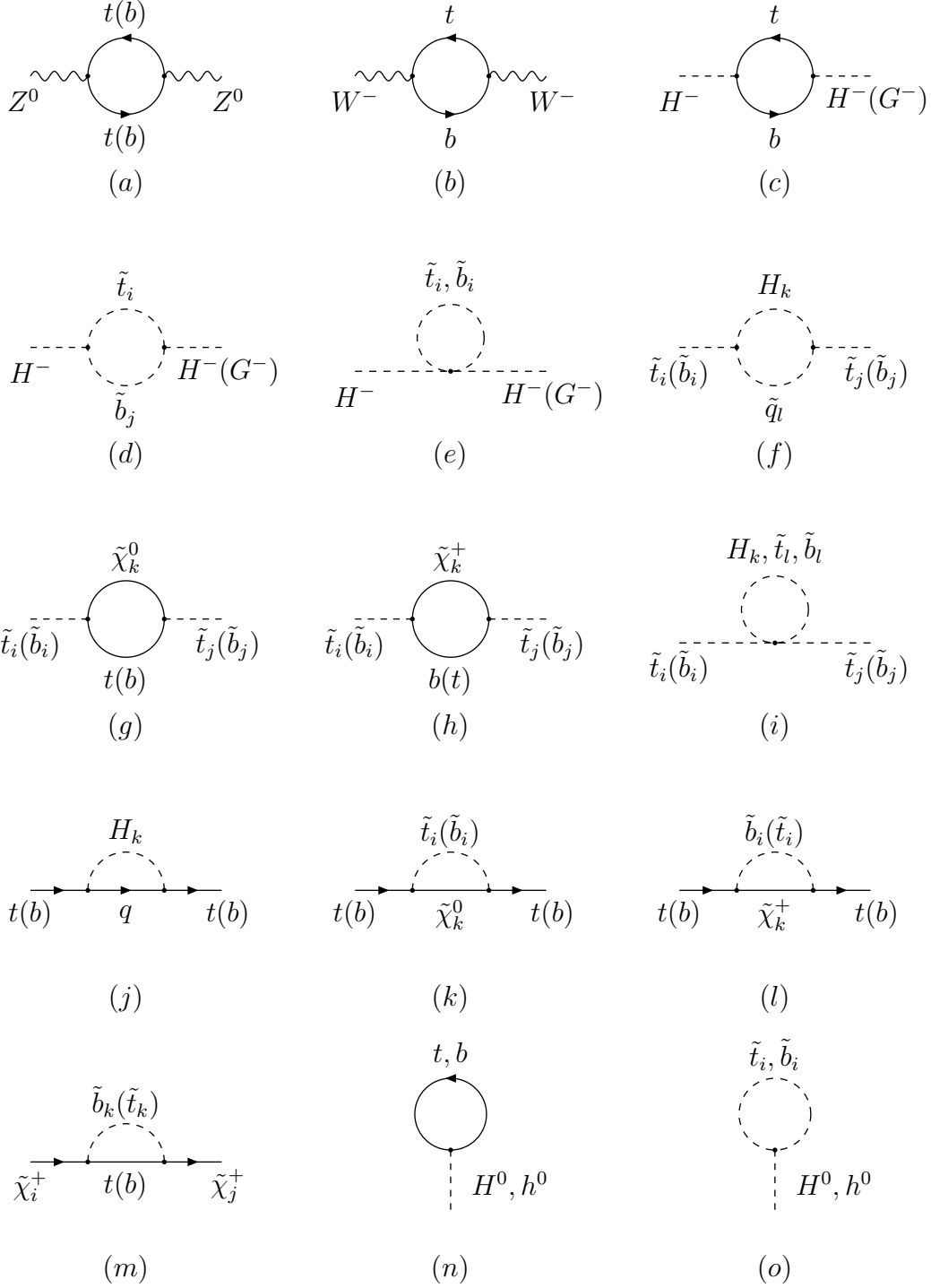


Figure 2: Feynman diagrams contributing to renormalization constants. In diagram (i) $q = t(b)$ for $k = 1 \dots 4$ and $q = b(t)$ for $k = 5, 6$.

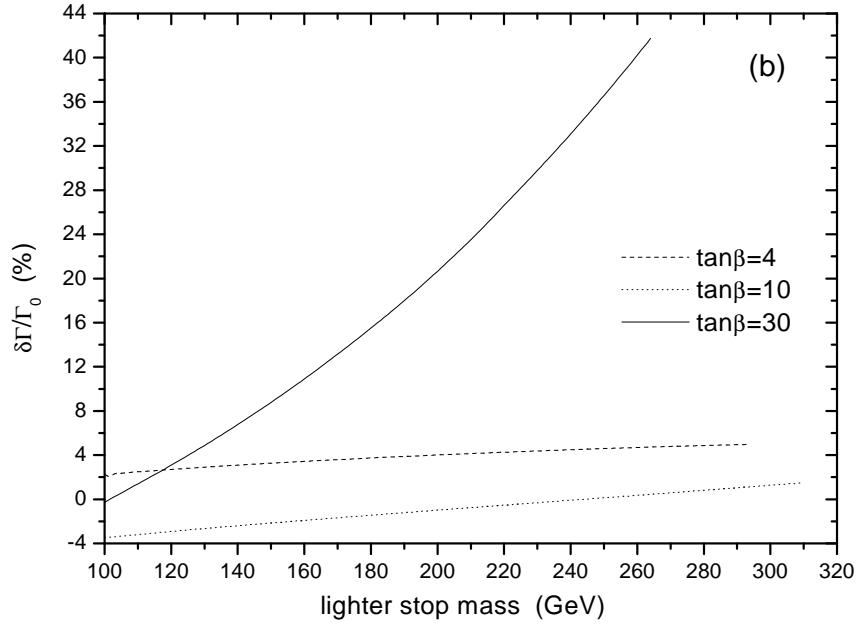
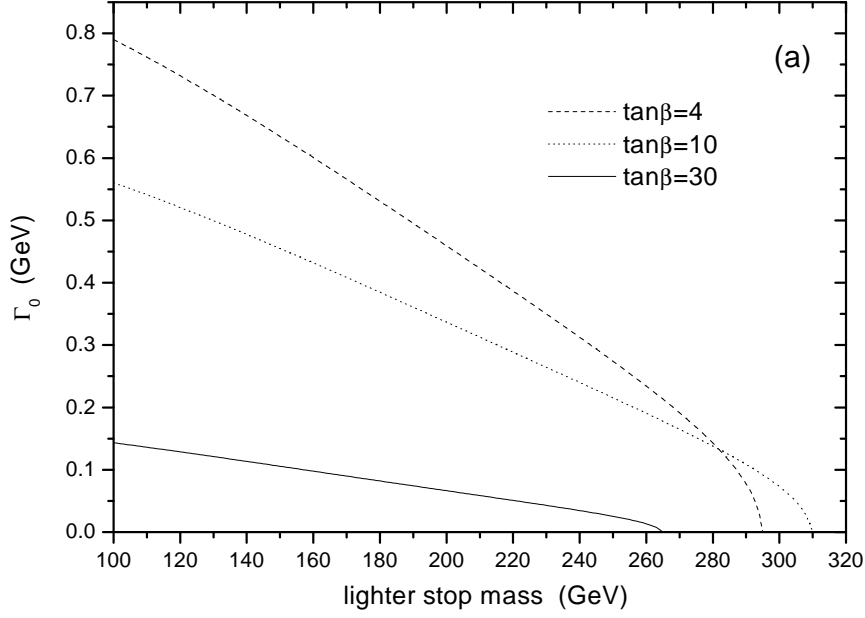


Figure 3: The tree-level decay width (figure (a)) of $\tilde{b}_1 \rightarrow \tilde{t}_1 H^-$ and its Yukawa corrections (figure (b)) as functions of $m_{\tilde{t}_1}$ for $\tan\beta = 4, 10$ and 30 , respectively, assuming $m_{A^0} = 150\text{GeV}$, $\mu = M_2 = 400\text{GeV}$, $A_t = A_b = 1\text{TeV}$ and $M_{\tilde{Q}} = M_{\tilde{U}} = M_{\tilde{D}}$.

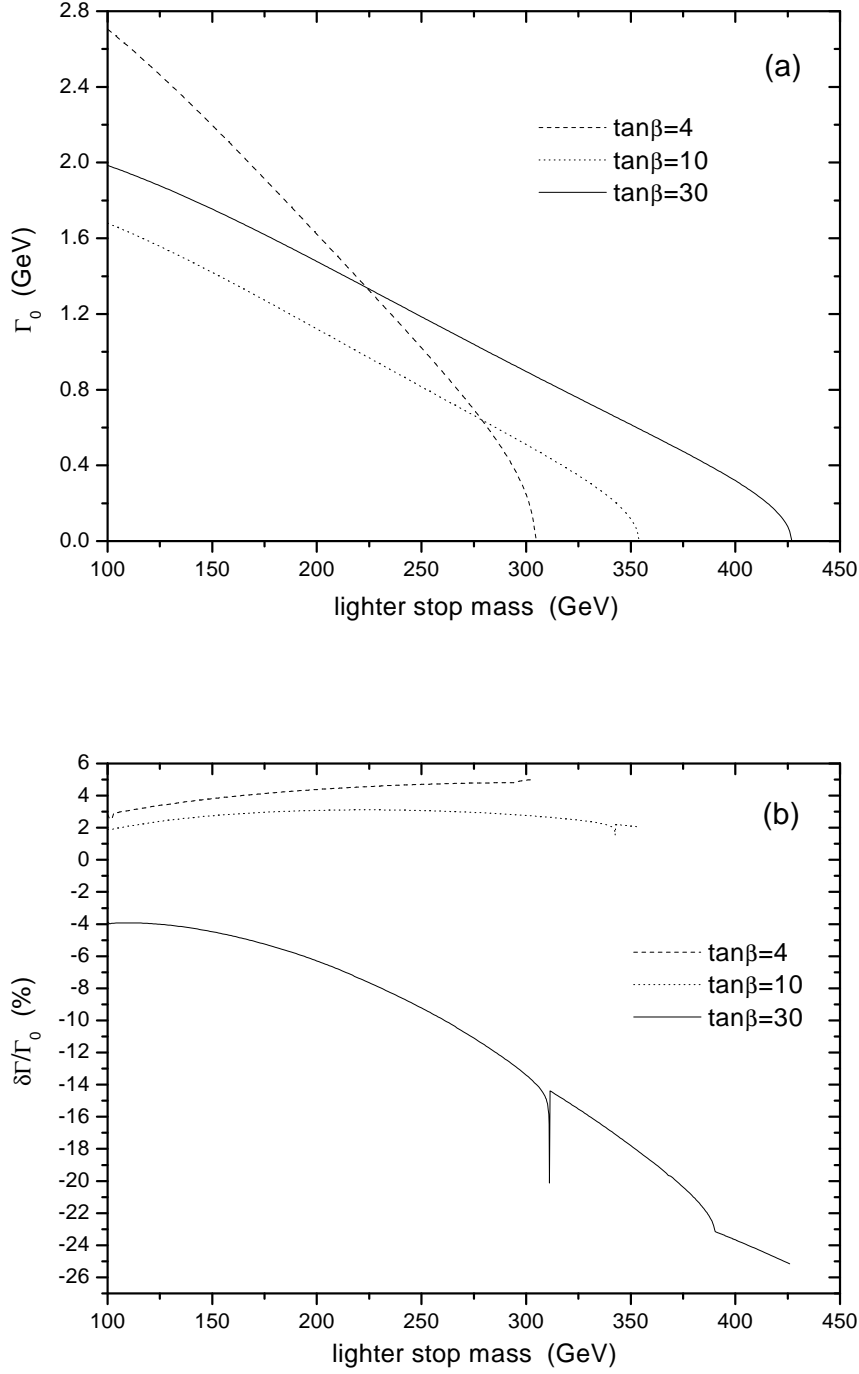


Figure 4: The tree-level decay width (figure (a)) of $\tilde{b}_2 \rightarrow \tilde{t}_1 H^-$ and its Yukawa corrections (figure (b)) as functions of $m_{\tilde{t}_1}$ for $\tan\beta = 4, 10$ and 30 , respectively, assuming $m_{A^0} = 150\text{GeV}$, $\mu = M_2 = 400\text{GeV}$, $A_t = A_b = 1\text{TeV}$ and $M_{\tilde{Q}} = M_{\tilde{U}} = M_{\tilde{D}}$.

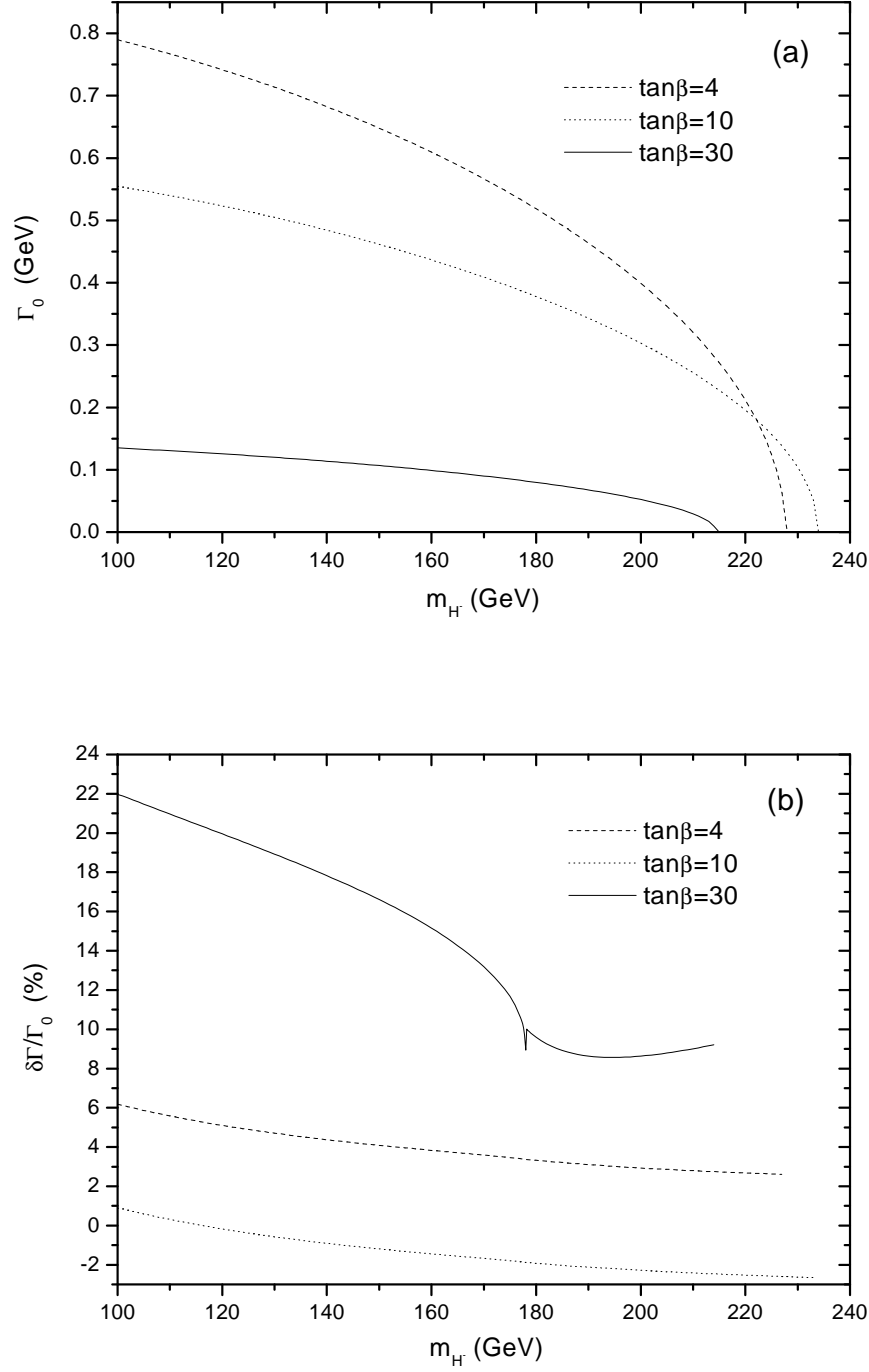


Figure 5: The tree-level decay width (figure (a)) of $\tilde{b}_1 \rightarrow \tilde{t}_1 H^-$ and its Yukawa corrections (figure (b)) as functions of m_{H^-} for $\tan\beta = 4, 10$ and 30 , respectively, assuming $m_{\tilde{t}_1} = 170\text{GeV}$, $\mu = M_2 = 400\text{GeV}$, $A_t = A_b = 1\text{TeV}$ and $M_{\tilde{Q}} = M_{\tilde{U}} = M_{\tilde{D}}$.

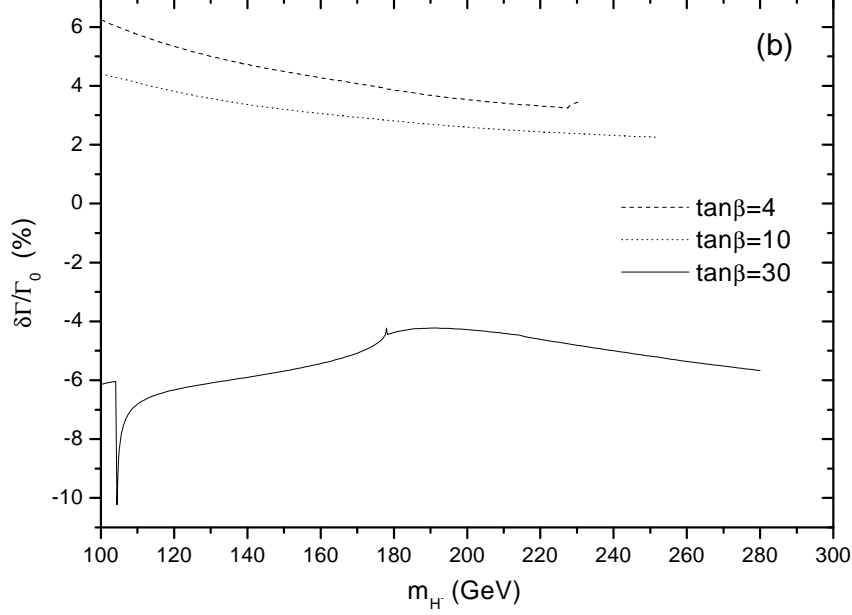
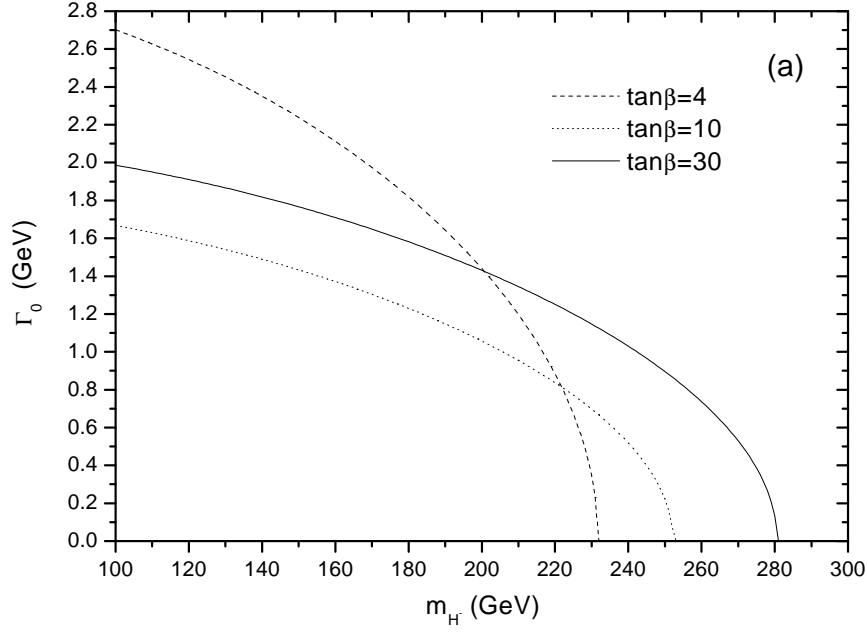


Figure 6: The tree-level decay width (figure (a)) of $\tilde{b}_2 \rightarrow \tilde{t}_1 H^-$ and its Yukawa corrections (figure (b)) as functions of m_{H^-} for $\tan\beta = 4, 10$ and 30 , respectively, assuming $m_{\tilde{t}_1} = 170\text{GeV}$, $\mu = M_2 = 400\text{GeV}$, $A_t = A_b = 1\text{TeV}$ and $M_{\tilde{Q}} = M_{\tilde{U}} = M_{\tilde{D}}$.

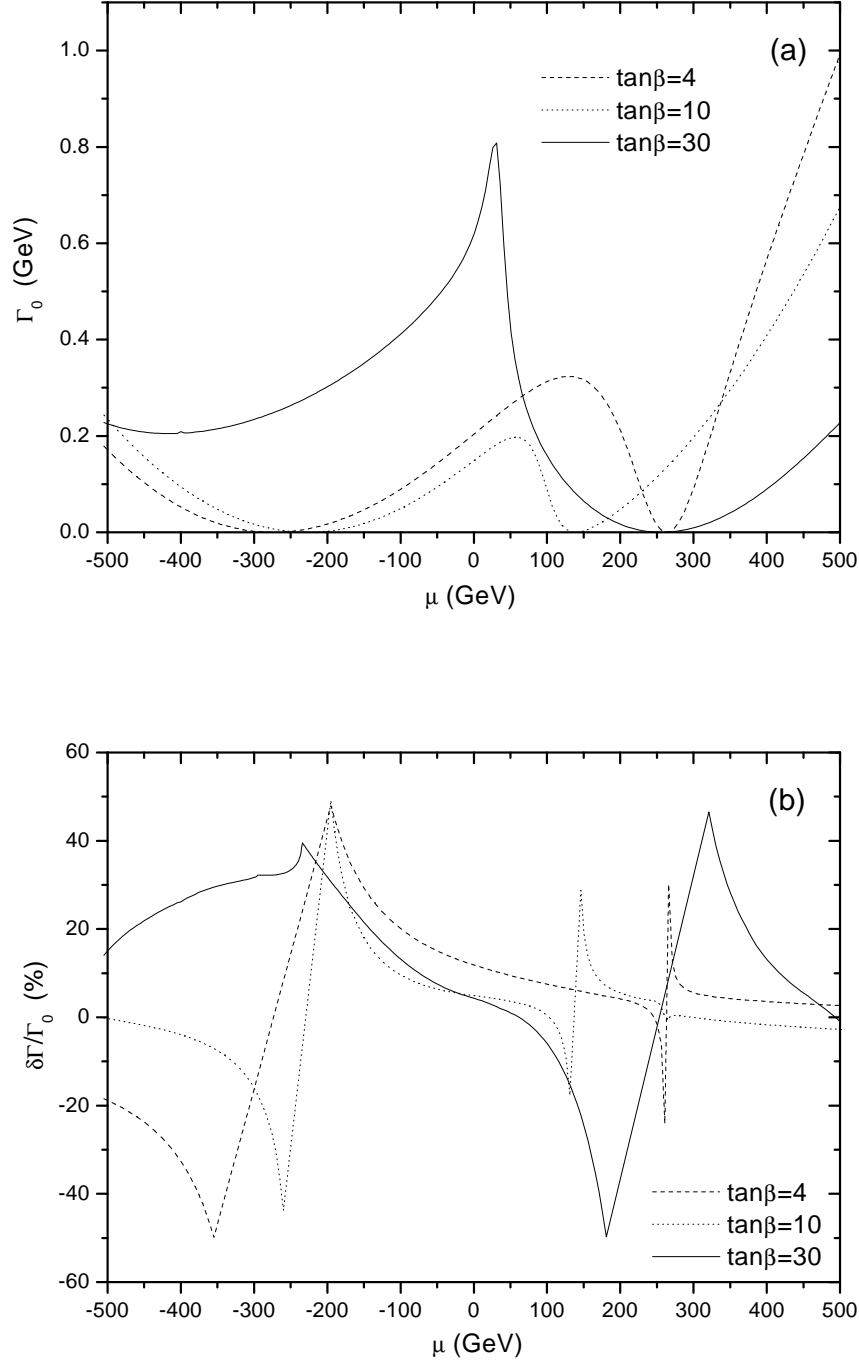


Figure 7: The tree-level decay width (figure (a)) of $\tilde{b}_1 \rightarrow \tilde{t}_1 H^-$ and its Yukawa corrections (figure (b)) as functions of μ for $\tan\beta = 4, 10$ and 30 , respectively, assuming $m_{\tilde{t}_1} = 170\text{GeV}$, $M_2 = 400\text{GeV}$, $A_t = A_b = 1\text{TeV}$, $m_{A^0} = 150\text{GeV}$ and $M_{\tilde{Q}} = M_{\tilde{U}} = M_{\tilde{D}}$.

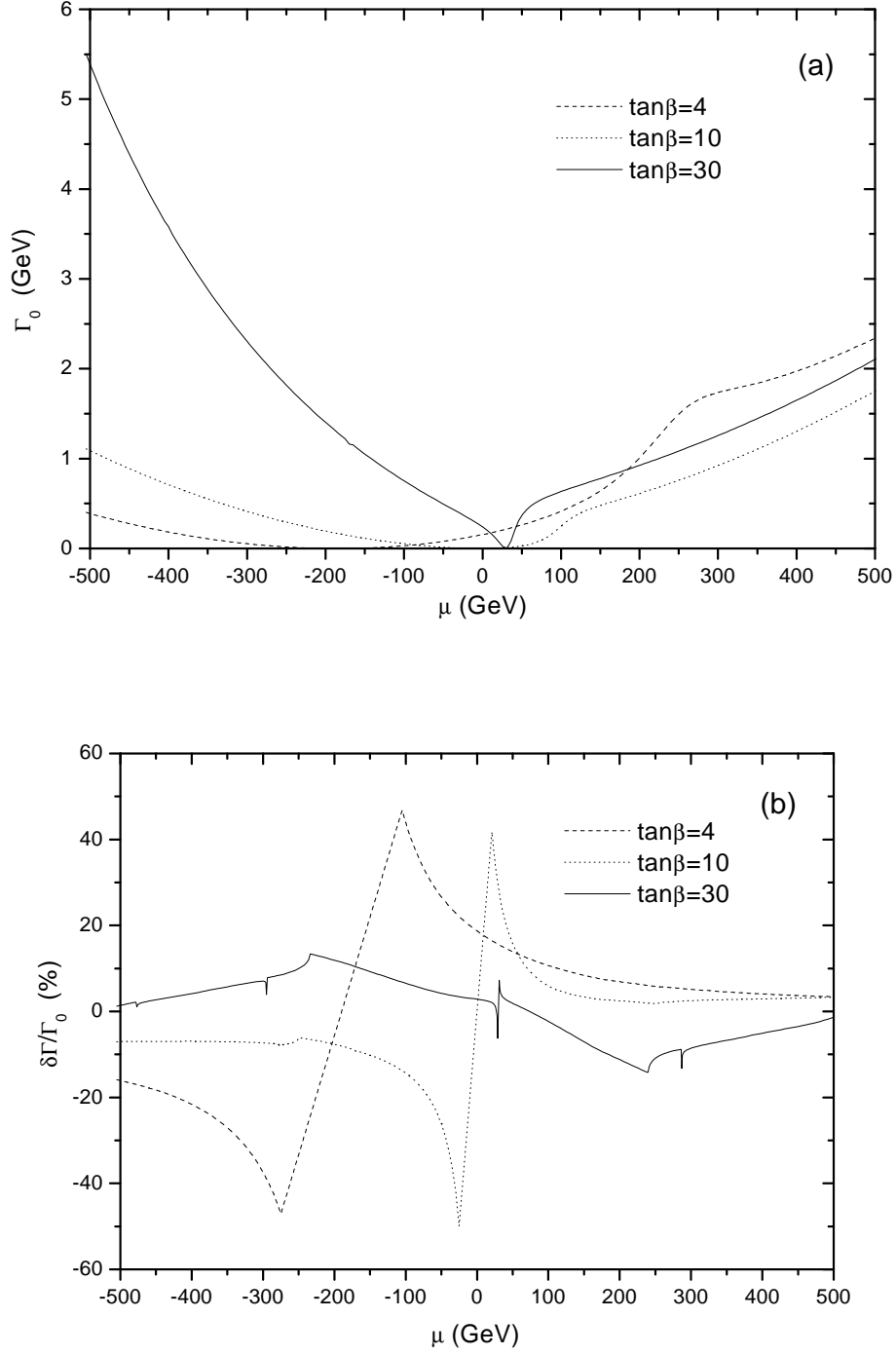


Figure 8: The tree-level decay width (figure (a)) of $\tilde{b}_2 \rightarrow \tilde{t}_1 H^-$ and its Yukawa corrections (figure (b)) as functions of μ for $\tan\beta = 4, 10$ and 30 , respectively, assuming $m_{\tilde{t}_1} = 170\text{GeV}$, $M_2 = 400\text{GeV}$, $A_t = A_b = 1\text{TeV}$, $m_{A^0} = 150\text{GeV}$ and $M_{\tilde{Q}} = M_{\tilde{U}} = M_{\tilde{D}}$.

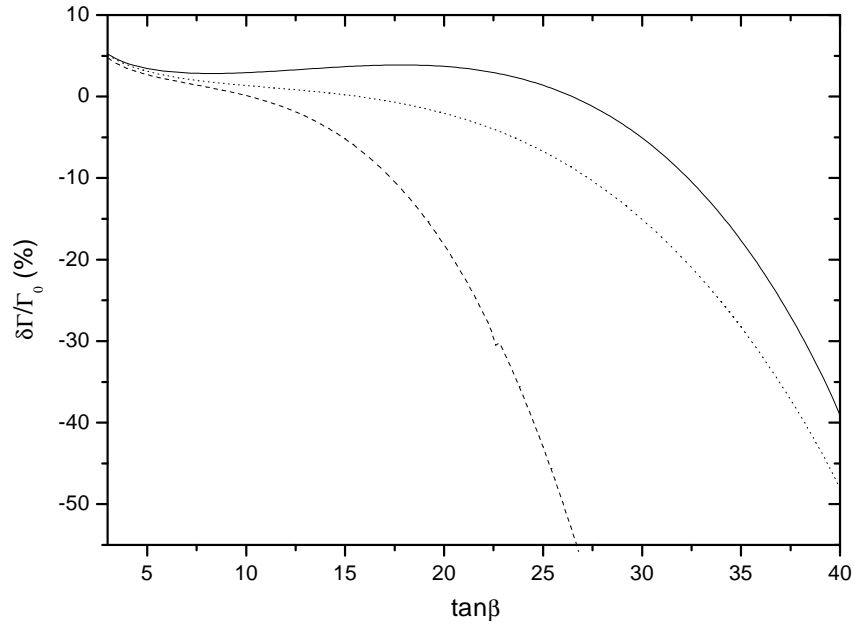


Figure 9: The Yukawa corrections of $\tilde{b}_2 \rightarrow \tilde{t}_1 H^-$ as a function of $\tan\beta$, assuming $m_{\tilde{t}_1} = 170\text{GeV}$, $\mu = M_2 = 400\text{GeV}$, $A_t = A_b = 1\text{TeV}$, $m_{A^0} = 150\text{GeV}$ and $M_{\tilde{Q}} = M_{\tilde{U}} = M_{\tilde{D}}$. The dashed line corresponds to the corrections using the on-shell bottom quark mass, the dotted line to the improved result only using the QCD running mass $m_b(Q)$, and the solid line to the improved result using the replacement Eq.(36).